Solid State Ionics 413 (2024) 116610

Contents lists available at ScienceDirect

Solid State Ionics

journal homepage: www.elsevier.com/locate/ssi

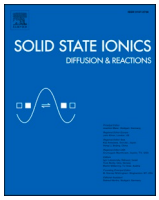

Effect of yttrium ion on the space charge potential across grain boundaries regions of gadolinia-doped ceria electrolytes

Eduarda Gomes [a], Devaraj Ramasamy [a,b], António A.L. Ferreira [a], João C.C. Abrantes [a,*]

[a] proMetheus, Instituto Politécnico de Viana do Castelo, 4900-347 Viana do Castelo, Portugal
[b] INL–International Iberian Nanotechnology Laboratory, 4715-330 Braga, Portugal

ARTICLE INFO

Keywords:
Low-grade
Scavenge
Electrolytes
Space charge
Hot press

ABSTRACT

In the present work, gadolinium-doped ceria-based powders were co-fired with additions of 1% (*w*/w) of SiO_2, and 5% (w/w) of Y_2O_3 to test the role of yttrium ion on improving the grain boundary conductivity across the grain boundary regions of low grade gadolinia-doped ceria (CGO) electrolytes. The samples were prepared by hot press at low temperature (1000 °C) to minimize bulk dissolution of yttrium in the CGO lattice. Structural characterization by XRD of the prepared ceramics confirms a CGO single phase material with the fluorite type structure. All the samples were characterized by impedance spectroscopy as a function of temperature in air, in order to de-convolute different microstructural contributions to the overall electrical behaviour. The results showed, as expected, that the presence of small amounts of impurity of silica reduces the total conductivity, when compared with pure CGO ceramic sample. The grain boundary resistance of these ceramics, under low operating temperatures, has a large effect on the total conductivity and is related, on one hand with the presence of a space charge layer created by the local segregation of trivalent rare earth elements, and the consequently depletion of oxygen vacancies, and on the other hand by the blocking effect of the silicon impurity. However, the obtained results show that addition of yttria increases total conductivity when compared with impure samples without yttria. This effect was related with the partial recover of specific grain boundary conductivity, suggesting a preferential location of Si and Y cations on grain boundaries. The space charge potential values, calculated using impedance data, provided an approach to the promoting effect of recovering grain boundary conductivity by the yttrium ion.

1. Introduction

The low-temperature operation of solid oxide fuel cells (SOFCs) is advantageous from several points of view such as operational stability, the use of cheaper raw materials and the use of more reliable seals and interconnecting materials [1]. The recommended use of low-grade ceramics, much cheaper than the high-purity oxides, has silica as the predominant constituent of the grain boundary region. Due to the presence of thin siliceous films, the grain boundary has a blocking effect to the transport of oxygen ions across the electrolyte.

Doped ceria is one of the most recognized oxide ion conductors in the intermediate temperature range (IT-SOFCs) and shows much higher ionic conductivity than that of the well-established yttria-stabilized zirconia (YSZ) [2,3]. Gadolinium (Gd) is considered to be one of the excellent dopants for cerium oxide electrolyte because of high oxide ion conduction at 400–700 °C [4]. The total conductivity of Gd doped ceria-based electrolytes is not only affected by the grain conductivity, but also controlled by the conductivity across the grain boundary regions. When exposed to high temperature conditions, the grain conductivity is dominant and determine the total conductivity. However, under lower operating temperatures, the grain boundary resistance has a large effect on the total conductivity [2,3,5].

The low grain boundary oxide ion conductivity in acceptor-doped ceria electrolyte has been related, on one hand with the presence of a space charge layer created by the local segregation of trivalent rare earth elements, and the consequently depletion of oxygen vacancies [6], and on the other hand by the blocking effect of the silicon impurity [7].

Currently, the need of develop SOFC towards lower operating temperatures, decreasing the grain boundary resistance of the electrolyte to improve total conductivity and energy conversion efficiency, is extremely important. In order to overcome this problem, investigations have been done by the addition of low concentration of co-dopants to

* Corresponding author.
E-mail address: jabrantes@estg.ipvc.pt (J.C.C. Abrantes).

https://doi.org/10.1016/j.ssi.2024.116610
Received 30 December 2023; Received in revised form 22 May 2024; Accepted 1 June 2024
Available online 11 June 2024

improve the grain boundary conductivity.

Similar studies to the well-established stabilized zirconia system were done with alumina additions to CGO ceramics, but the results showed a detrimental effect, attributed to the formation of another non-conductive phase, $GdAlO_3$ [8]. Another attempt with CGO ceramics involved additions of lanthanum oxide, as scavenging agent, which proved to be effective on removing the siliceous phases from the grain boundaries [9].

It has also been reported that some transition metal oxides are effective aids both for the densification and improvement of the grain boundary behaviour of ceria-based electrolytes. Several metal oxides have been used to eliminate the space charge layer or to clean the silicon impurity phase in doped ceria electrolytes, such as Fe_2O_3 [10], ZnO [11] and NiO [12].

The effect of addition of alkalis was also investigated and was observed an improvement in the grain boundary conduction of ceria-based electrolytes containing a trace amount of SiO_2. However, few reports are available on the mechanism underlying the grain boundary impurity scavenging effect. Contradictory reports are available for the same cation dopant, for example, magnesium ion (Mg^{2+}) has been reported to scavenge the highly resistive siliceous phase [13] and to weaken the effect of the grain size on the grain boundary resistivity [14]. Studies of the addition of SrO suggest an enhancement of the grain boundary conduction of electrolytes via the scavenging effect [15–17] and also decreasing the space charge potential [18]. The effect of CaO addition in Gd-doped ceria was examined by Cho et al. and, in this case, attributed the improvement in conductivity to the configuration change in the grain boundary owing to segregation of CaO [19]. However, recently, Preethi and Babu demonstrated that Ca^{2+} and Sr^{2+} ions effectively scavenges the silicious phase and space charge region by lowering its potential in samarium doped ceria electrolyte [20]. In the same work, Preethi and Babu concluded that the scavenging effect of other alkaline earth ions revealed that Ba^{2+} is unstable, causing a high strain, and Mg^{2+} induce large compression stress, leading to its segregation at grain boundaries [20]. In a previous work, Park et al. had suggested that BaO seems to play dual roles in the grain-boundary conduction of gadolinium doped ceria, by deteriorating it at low concentration, and dramatically enhancing it at high concentration [21].

Recently, Sun et al. reported that the scavenging effect of Sr^{2+} ion on gadolinium doped ceria is only effective when the sintering temperature is higher than the eutectic temperature of the Si grain boundary impurities [22].

In a similar study, Ge et al. reported a strategy of "scavenger promoter" through a synergy between co-additions of CaO and ZnO in the samarium doped CeO_2, with ZnO being assigned to promote the scavenging reaction between CaO and SiO_2 [23].

So far, there are few reports about the effects of doping with monovalent alkali metals (Li, Na, K) on grain boundary conduction. However, in a recent work, Song et al. showed that the monovalent alkali metals dopants (Li, Na, K) have promoting effects on densification and on improving the grain boundary conductivity owing to the observed decrease of space charge potential [24].

Although has been proved that transition metals and alkaline earth metals doping improve the grain boundary behaviour, a series of drawbacks have also been identified. Transition metal doping may cause electron conduction of electrolyte, which will cause a short circuit in the cell and affect the electrochemical performance [25]. Furthermore, many transition metals are toxic materials, causing environmental pollution and being not suitable for long-term energy development. Also, alkaline earth metals dopants show poor stability property in CO_2 atmosphere, leading to degradation of the components of SOFCs [26].

Kim et al. reported an increase in conductivity by multiple doping of yttrium, lanthanum, samarium, neodymium and gadolinium in ceria. This improvement was identified to be caused by an increase in configurational entropy of the system [27].

In this study 1% (*w*/w) of silica is intentionally added to the $Ce_{0.95}Gd_{0.05}O_{2-\delta}$ (CGO5) system to simulate silica contamination and is exploited an alternative approach using the addition of 5% (*w*/w) of Y_2O_3 as silica scavenging agent. Non-conventional sintering, such hot pressing at low temperature, was used to obtain dense ceramics and minimizing bulk dissolution of yttrium in the CGO lattice.

2. Experimental

Commercially available $Ce_{0.95}Gd_{0.05}O_{2-\delta}$ (CGO5) (Praxair), SiO_2 (Sibelco P500) and Y_2O_3 (Alfa Aesar) high purity powders were used as starting materials. CGO5 was used as a reference material to compare with the following compositions: CGO5 + 1%(*w*/w) SiO_2 and CGO5 + 1%(w/w) SiO_2 + 5% (w/w) Y_2O_3. All compositions were prepared using conventional ceramic processing route, mixing powders with ethanol in a ball mill with zirconia milling media. The slurries obtained were dried. The obtained powders were uniaxially pressed into cylindrical pellets. In order to obtain dense ceramics, the pellets of each composition were sintered in a variety of conditions: hot press sintering at 1000 °C for 2 h with 65 MPa; hot press sintering at 1000 °C for 2 h followed by a thermal treatment at 1100 °C for 2 h; hot press sintering at 1000 °C for 2 h followed by a thermal treatment at 1400 °C for 2 h. The notation used, the composition and the thermal treatment of each sample prepared is presented in Table 1.

Sintering process was performed in air with a constant heating rate of 5 °C/min and cooling rate of 5 °C/min. The density of each sample was calculated using Archimedes method. The samples were analysed by x-ray diffraction (XRD) and scanning electron microscopy with energy dispersive spectroscopy (SEM/EDS).

The bulk and grain boundary resistances were obtained by ac impedance spectroscopy in air using Hewlett-Packard 4284 A Impedance Analyzer. Pt electrodes were applied on both surfaces of the pellet and fired at 1000 °C. The electrical measurements were performed from 1000 °C to 100 °C, in the frequency range of 20 Hz -1 MHz.

3. Results and discussion

3.1. Structural and microstructural analysis

X-ray difraction analysis was carried out to identify the dissolution of the co-dopants in ceria lattice. Fig. 1 shows XRD patterns of the prepared ceramic samples. The observed diffraction peak positions (2θ) confirmed the formation of cubic fluorite structured with a primitive space group of $Fm\bar{3}m$ (ICDD card no.04016–6473) without the formation of any secondary phase. The slight increase of the lattice parameter (a_0) (Table 1) also suggests the formation of solid solution.

The size of unit cells of the samples with Si and Y decreased slightly with an increase in the temperature of thermal treatment when

Table 1
Prepared samples notation, composition, thermal treatment, and obtained relative density (RD) and lattice parameter (a_0).

Sample	Composition	Thermal treatment	RD (%)	a_0 (Å)
CGO5	$Ce_{0,95}Gd_{0,05}O_{2-\delta}$	HP	92.42	5.4165 ± 0.0002
CGO5 Si	$Ce_{0,95}Gd_{0,05}O_{2-\delta}$ + 1%(w/w) SiO_2	HP	77.56	5.4177 ± 0.0004
CGO5 Si 1100	$Ce_{0,95}Gd_{0,05}O_{2-\delta}$ + 1%(w/w) SiO_2	HP + 1100 °C 2 h	93.36	5.4157 ± 0.0002
CGO5 Si 1400	$Ce_{0,95}Gd_{0,05}O_{2-\delta}$ + 1%(w/w) SiO_2	HP + 1400 °C 2 h	95.97	5.4140 ± 0.0001
CGO5 Si 5Y	$Ce_{0,95}Gd_{0,05}O_{2-\delta}$ + 1%(*w*/w) SiO_2 + 5% (*w*/w) Y_2O_3	HP	83.97	5.4172 ± 0.0003
CGO5 Si 5Y 1100	$Ce_{0,95}Gd_{0,05}O_{2-\delta}$ + 1%(w/w) SiO_2 + 5% (w/w) Y_2O_3	HP + 1100 °C 2 h	85.44	5.4141 ± 0.0002
CGO5 Si 5Y 1400	$Ce_{0,95}Gd_{0,05}O_{2-\delta}$ + 1%(w/w) SiO_2 + 5% (w/w) Y_2O_3	HP + 1400 °C 2 h	93.44	5.4127 ± 0.0001

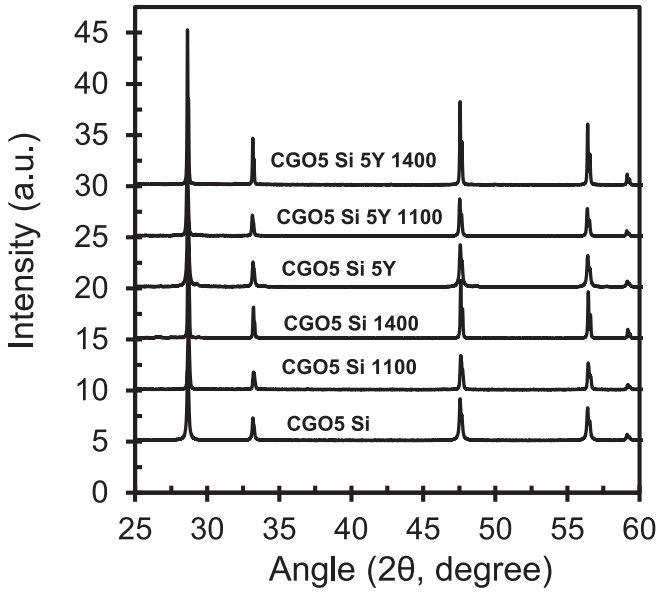

Fig. 1. XRD patterns of the prepared ceramic samples.

comparing the samples obtained only by hot press with the samples obtained by hot press followed by a thermal treatment at 1100 °C (Fig. 2), which could be related with a higher incorporation inside the lattice of CGO of a smaller ion of Si^{4+}, whose ion radius ($R = 0.41$ Å) is smaller than that ion radius of Ce^{4+} ($R = 0.97$ Å), and also the ion Y^{3+}, whose ionic radius ($R = 1.019$ Å) is slightly lower than the ionic radius of Gd^{3+} ($R = 1.050$ Å) [28]. However, the increase of lattice parameter observed with increase in the temperature of thermal treatment within the material of reference CGO5, may be related with the reduction of Ce^{4+} to Ce^{3+} observed at higher temperatures [29] suggesting that this effect freeze during the cooling process to the room temperature.

SEM/EDS analysis also showed a homogeneous distribution of Si and Y over all the samples, suggesting an incorporation of this elements into the CGO lattice. The microstructures of samples obtained by hot press are submicrometric as revealed, for instances, by the SEM micrograph of CGO5 Si 5Y (Fig. 3). The chemical quantification obtained by EDS of this

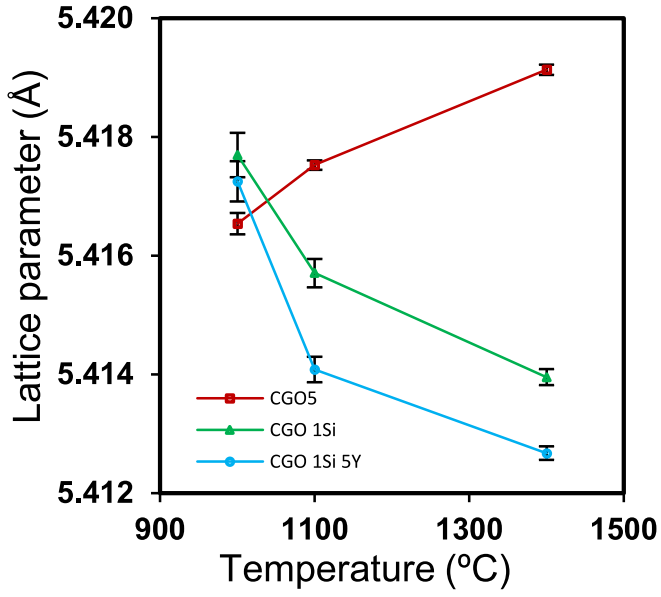

Fig. 2. Variation of the lattice parameter of the prepared ceramic samples with the thermal treatment.

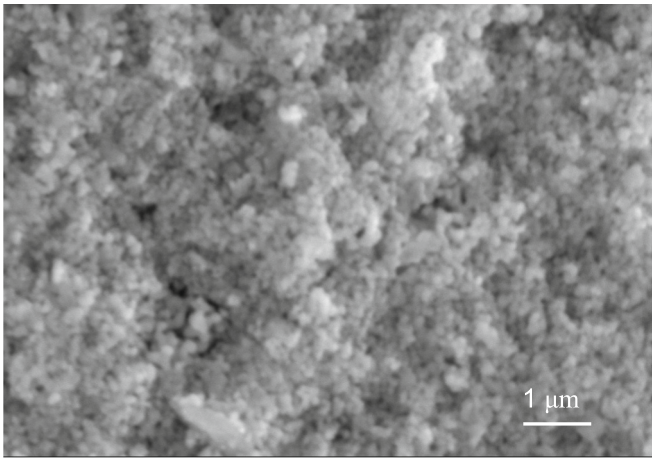

Fig. 3. SEM micrography of sample CGO5 Si 5Y.

sample confirms the theoretical elementary composition of the CGO5 (Table 2). However, there is a difference within the values obtained for the elements Si and Y, probably related to the low representativeness of the analysed fraction of the sample and to the accuracy of the technique in quantifying low concentration of elements. Elementary quantification by EDS aimed to identify eventual microstructural heterogeneities near the grain boundaries, particularly in the distribution of Si and Y, but this was not detected.

3.2. Electrical characterization

Fig. 4 shows the impedance spectra of the samples CGO5, CGO Si and CGO Si 5Y obtained at 600 °C, showing a clear improvement in the impedance of the sample with addition of yttria. A typical impedance spectrum could be divided into three regions: (1) a high frequency arc ascribed to bulk polarisation, (2) an intermediate-frequency arc corresponding to grain boundary polarisation, and (3) a low-frequency arc attributed to electrode polarisation, which was absent in Fig. 4 because it was beyond the limit of the equipment used in this study. The fitted results were consistent with the plots. Ideally, the frequency response of polycrystalline doped ceria can be modelled by a resistor and a lossy capacitor in parallel, and the capacitance can be calculated as [18]:

$$\omega = \frac{1}{RC} \quad (1)$$

where C is the bulk or grain boundary capacitance, R is the bulk or grain boundary resistance, and ω is the frequency of maximum loss in the impedance spectrum. However, considering the microstructural inhomogeneity of the samples used in this study, the loss capacitor was replaced by a constant phase element (CPE), and the impedance spectra were fitted using the software *ISA* [30] with the configuration ($R_{bulk}CPE_{bulk}$) ($R_{gb}CPE_{gb}$), where R_{bulk} refers to the bulk resistance and R_{gb} refer to the grain boundary resistance, respectively.

The bulk and grain boundary conductivities were calculated using the following equation

Table 2
Chemical quantification of the sample CGO5 Si 5Y theoretical and obtained by EDS.

Element	Theoretical (at.%)	EDS (at.%)
Ce	31.20	31.84
Gd	1.64	1.72
O	64.04	64.06
Si	0.85	1.57
Y	2.27	0.81

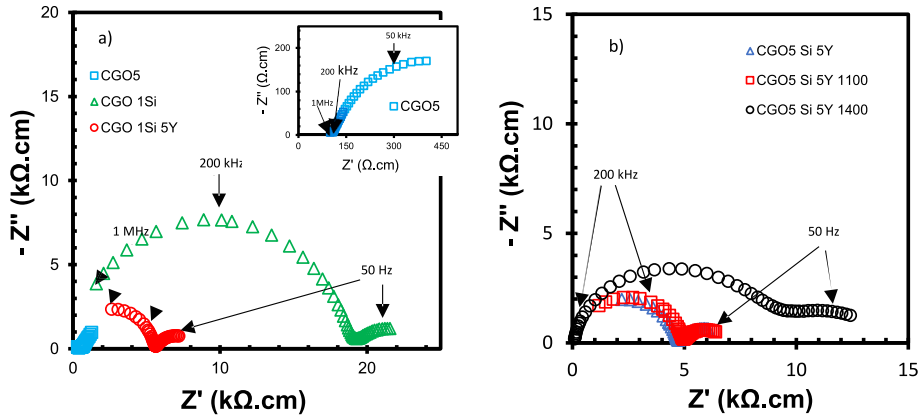

Fig. 4. Typical impedance spectra obtained at 600 °C for different compositions on a) and thermal treatment temperature effect on b). The arrows correspond to the frequency at the given points.

$$\sigma = \frac{L}{AR} \tag{2}$$

where L, A and R are the thickness of the pellet, the electrode area on the sample surface and the resistance of bulk or grain boundary, respectively.

The specific grain boundary conductivity (σ^s_{gb}) is likely to indicate whether the nature of grain boundaries and their properties are significantly dependent on composition. In this study, was taken into account that the effective area to thickness ratio $(A/t)_{eff}$ plays opposite effects on the grain boundary capacitance and grain boundary resistance [31]. These effects cancel in the peak relaxation frequency $f_{gb} = \left(2\pi C_{gb} R_{gb}\right)^{-1} = \frac{\sigma_{gb}}{2\pi\varepsilon_0\varepsilon_r}$ and thus specific grain boundary conductivity become

$$\sigma^s_{gb} = 2\pi f_{gb}\varepsilon_0\varepsilon_r \tag{3}$$

where $\varepsilon_0 = 8.854 \times 10^{-12}$ F is the permittivity of vacuum, and the dielectric constant $\varepsilon_r = 30$ was obtained from literature data [32].

The activation energy was calculated using an Arrhenius equation, taking into account the Nernst-Einstein relation for ionic diffusion:

$$\sigma T = \sigma_0 exp\left(-\frac{E}{kT}\right) \tag{4}$$

where σ_0 is the pre-exponential factor, E is the activation energy (eV), T is the absolute temperature (K) and k is the Boltzmann's constant. The slope of ln scale of Arrhenius equation gives the activation energy required for the ionic conductivity in each of the samples. Arrhenius plots for bulk, grain boundary and total conductivities for all the samples prepared were obtained from the conductivity data.

Table 3 lists the activation energy for bulk (E_g) and grain boundary (E_{gb}) conductivity of the samples prepared without and with different thermal treatments, which, in the case of the reference material CGO5, are in good agreement with the values obtained elsewhere for the activation energy measured in Gd-doped ceria ceramics upon change in the dopant concentration [33].

Table 3
Bulk and grain boundary activation energy of sintered pellets calculated in the range 100–300 °C and 300–700 °C, respectively.

Sample	E_g (eV)	E_{gb} (eV)
CGO5	0.70 ± 0.09	1.00 ± 0.22
CGO5 Si	0.68 ± 0.07	1.30 ± 0.17
CGO5 Si 1100	0.67 ± 0.03	1.45 ± 0.07
CGO5 Si 1400	0.68 ± 0.01	1.36 ± 0.08
CGO5 Si 5Y	0.65 ± 0.07	1.19 ± 0.05
CGO5 Si 5Y 1100	0.71 ± 0.06	1.14 ± 0.05
CGO5 Si 5Y 1400	0.78 ± 0.02	1.40 ± 0.16

The activation energy for oxide ions conductivity in the bulk increase with increase in thermal treatment temperature for samples with only silica and for samples with silica and yttria. This is in agreement with a higher incorporation of Si^{4+} and Y^{3+} ions in the CGO lattice, contracting the lattice as described in XRD and hence making difficult the oxygen ion conductivity. In fact, was shown that when density increases, the average activation energy for oxygen ion conduction decreases [34]. Even though, vacancy concentration increases and thus addition of Y^{3+}, besides contracting the lattice, seems to raise the binding energy of lattice trapping the free oxygen vacancies [16,35].

E_{gb} was higher than the Eg for all the samples, with additions of silica and additions of silica and yttria, when compared with the value of the sample CGO5, due to the grain boundary blocking effect. These blocking effects are usually ascribed to the presence of silicious impurity and a space charge region [36]. The silicious impurity segregates to the grain boundary and forms a thin film which hinders the oxygen ion migration. Also, it is well agreed from the literature that the grain boundary core is positively charged probably due to the enrichment of oxygen vacancies. This creates an electrostatic potential barrier between the grain boundary core and the adjacent grain. In order to compensate this charge, oxygen vacancies were depleted in the adjacent grain space charge layer. This depletion of oxygen vacancies hinders the hopping of mobile oxygen ions, which, in turn, increases E_{gb} [32,36].

The addition of silica to the reference material CGO5 increases the E_{gb} from 1.0 eV to 1.3 eV. This effect of addition of silica was not observed within the system $Ce_{0.8}Sm_{0.2}O_{1.9}$ [23], probably because in this work the sintering process was done at very high temperature (1600 °C) [36], in opposition with the low temperature of hot press sintering used in the present work, leading to a different distribution of Si ion along the microstructure of prepared samples.

The E_{gb} of samples CGO5 Si 5Y and CGO5 Si 5Y 1100 (1.19 and 1.14 eV, respectively) are lower when compared with the samples without yttria and with the same thermal treatment (1.3 eV for CGO5 Si and 1.45 eV for CGO5 Si 1100), suggesting that the presence of Y^{3+} near the grain boundary core act as a negative defect and neutralises the excess positive charge. This effect reduces the potential barrier and, consequently, increases the oxygen vacancy concentration along the grain boundary space-charge layer, leading to a reduced E_{gb} compared with CGO5 Si with the same thermal treatment. However, this effect is not observed when comparing the samples CGO5 Si 5Y1400 and CGO5 Si1400, suggesting that at such high temperatures the ions Si^{4+} and Y^{3+} are incorporated into the grain, thus leading to opposite effects in the values of E_{gb}.

Fig. 5 shows the Arrhenius plots of total and bulk conductivities of samples prepared with different thermal treatments. Fig. 5.a) shows that

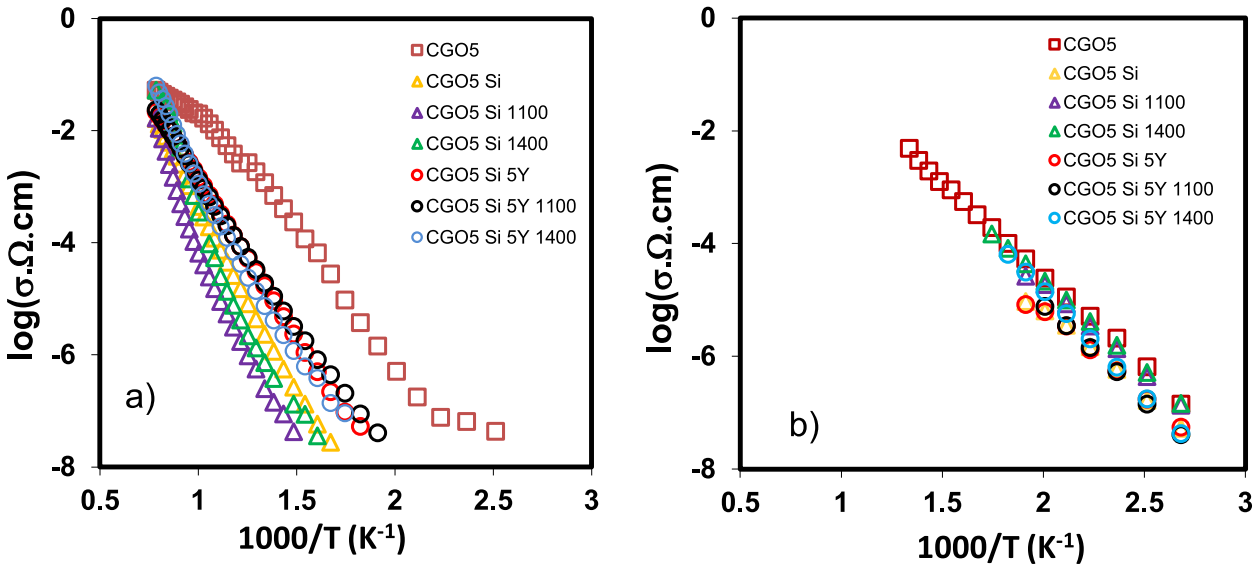

Fig. 5. Arrhenius plots of total (a) and bulk (b) conductivities of samples prepared with different thermal treatments.

addition of silica decreases that total conductivity when compared with the sample without silica, and this behaviour is observed for all thermal treatments. The lowest total conductivity is obtained for the sample CGO5 Si 1100. The total conductivity is partially recovered with simultaneous additions of silica and yttria and the higher value was obtained with the sample CGO5 Si 5Y 1100. Fig. 5.b) shows the Arrhenius plot of bulk conductivity of all the samples. The samples with additions of silica and yttria shows the lowest values of bulk conductivity, showing that although doping with Y^{3+} increase the oxygen vacancy content, oxide ion conductivity decrease.

The Arrhenius plots of apparent grain boundary conductivity of samples with different thermal treatments (Fig. 6.a) shows the detrimental effect of silica and the improvement effect of yttria. In fact, the specific grain boundary conductivity increases with the addition of yttria when comparing with the sample with the only addition of silica (Fig. 6.b). Si ion significantly decrease the specific grain boundary conductivity, which suggests the presence of this impurity on the grain boundaries. However, the specific grain boundary conductivity is partially recovered with the addition of yttria for all temperatures of thermal treatment (Fig. 7).

To quantitively analyse the effect of yttrium ion on the grain boundaries behaviour, similarly to the approach considered by other authors [21,37], the recover factor of yttrium ion (*RF*) was calculated using eq. 5 for each thermal treatment. *RF* is the ratio between the specific grain boundary resistivity before scavenging (ρ_{bs}^{sp}), corresponding to the samples with addition of silica, and the specific grain boundary resistivity after scavenging (ρ_{as}^{sp}), corresponding to the samples with addition of silica and yttria. This factor is more than one order of magnitude higher for the thermal treatment at 1100 °C when compared with the other thermal treatment temperatures. These values were obtained for the temperature of 500 °C, which besides belonging to the intermediate range of temperatures under prospective working conditions, also allows the characterization of the grain boundary contribution. The recovering effect of yttrium ion can be attributed to a decrease in space-charge potential, $\Delta\varphi_0$, or a decrease in the grain boundary coverage proportion.

$$RF = \frac{\rho_{bs}^{sp}}{\rho_{as}^{sp}} \tag{5}$$

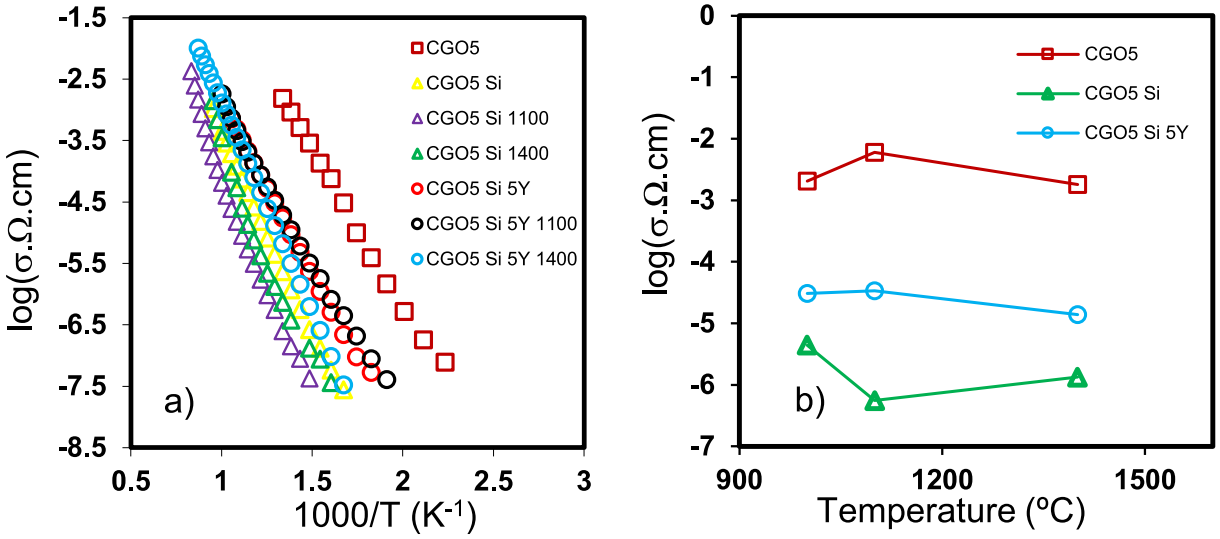

Fig. 6. Arrhenius plot of (a) apparent grain boundary conductivity of samples with different thermal treatments and (b) specific grain boundary conductivity at 500 °C of samples of CGO5, samples with only addition of silica, and samples with silica and yttria, as a function of thermal treatment temperature.

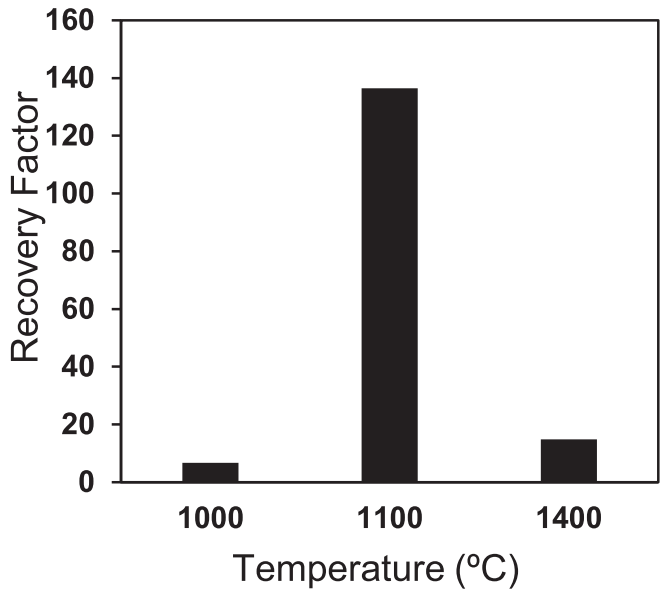

Fig. 7. Recovery factor as a function of thermal treatment temperature measured at 500 °C.

The value of $\Delta\varphi_0$ was estimated as follows:

$$E_{gb} - E_g = (2e\Delta\varphi_0 - k_B T) \quad (6)$$

where e is the elementary electrical charge, k_B is the Boltzmann constant and T is temperature [38].

In fact, it was observed that Si ion significantly increases the space charge potential (Fig. 8), causing depletion of oxygen vacancies, and thus contributing to the observed reduction in grain boundary conductivity.

On the contrary, yttrium ion reduces the space charge potential, reversing the negative effect of silica, being the lower space charge value obtained to the thermal treatment at 1100 °C. This is consistent with the observed higher value of the recovery factor obtained for the temperature of 1100 °C. Increasing the thermal treatment temperature to 1400 °C, is observed an increase of the space charge of sample with yttria addition, related with the incorporation of Y^{3+} from the grain boundaries into the bulk (Fig. 8), suggesting that the Y ion content at grain boundaries is an important factor in the scavenge effect, as observed and represented on Fig. 7.

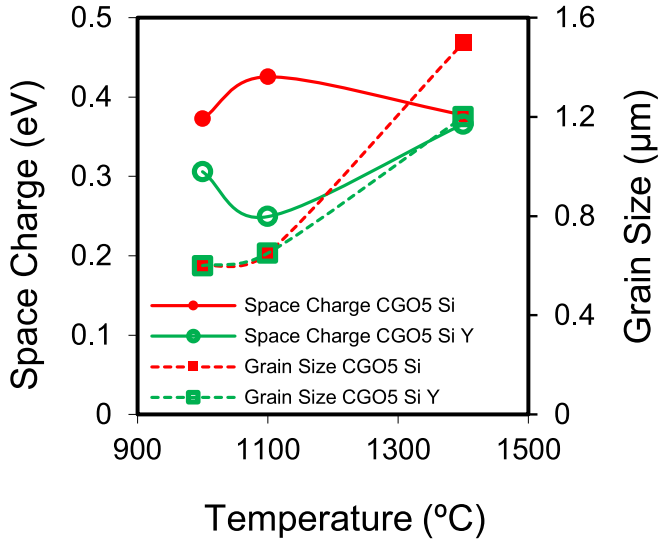

Fig. 8. Graphic representation of space charge and grain size effects for the samples with addition of silica and addition of silica and yttria for different thermal treatment temperatures.

Fig. 8 also shows that an increase in thermal treatment temperature raises the average grain size. The effect of an increase in grain size has been related to an enhancement in the grain boundary impurity coverage proportion by decreasing the grain boundary area [39]. In this study, although has been observed an increase in the average grain size within the thermal treatment temperature of 1400 °C, the effect of impurity coverage proportion seems to be contradictory, as the space charge potential of the sample with only addition of silica and thermal treated at 1400 °C slightly decreases when compared with the same composition thermal treated at 1100 °C (Fig. 8). This also suggests the dissolution of silica ion into the bulk, in agreement with the slight increase in the specific grain boundary conductivity observed for this sample (Fig. 6.b).

4. Conclusions

Samples of gadolinium-doped ceria-based electrolytes were thermal treated at different temperatures (1100 and 1400 °C) after hot press at 1000 °C. High density (≥90%) was achieved with almost all the samples.

Addition of small amounts of impurity of silica showed a strong effect in decreasing the total conductivity when compared with pure ceramic sample.

However, addition of yttria increased the total conductivity when compared with samples without yttria. This effect was more effective with the thermal treatment of 1100 °C.

Yttrium, when located at the grain boundaries, improve its specific conductivity and its content seems to play an important role in the scavenge effect.

Ethical Statement for Solid State Ionics

Hereby, I João C.C. Abrantes consciously assure that for the manuscript *Effect of yttrium ion on the space charge potential across grain boundaries regions of gadolinia-doped ceria electrolytes* the following is fulfilled:

1) This material is the authors' own original work, which has not been previously published elsewhere.

2) The paper is not currently being considered for publication elsewhere.

3) The paper reflects the authors' own research and analysis in a truthful and complete manner.

4) The paper properly credits the meaningful contributions of co-authors and co-researchers.

5) The results are appropriately placed in the context of prior and existing research.

6) All sources used are properly disclosed (correct citation). Literally copying of text must be indicated as such by using quotation marks and giving proper reference.

7) All authors have been personally and actively involved in substantial work leading to the paper, and will take public responsibility for its content.

The violation of the Ethical Statement rules may result in severe consequences.

To verify originality, your article may be checked by the originality detection software iThenticate. See also http://www.elsevier.com/editors/plagdetect.

I agree with the above statements and declare that this submission follows the policies of Solid State Ionics as outlined in the Guide for Authors and in the Ethical Statement.

Date: December, 29th.

CRediT authorship contribution statement

Eduarda Gomes: Writing – original draft, Methodology, Investigation, Formal analysis, Data curation, Conceptualization. **Devaraj Ramasamy:** Investigation, Data curation. **António A.L. Ferreira:** Methodology, Investigation, Conceptualization. **João C.C. Abrantes:** Writing – review & editing, Supervision, Resources, Project administration, Methodology, Funding acquisition, Formal analysis, Data curation, Conceptualization.

Declaration of competing interest

The authors declare that they have no known competing financial interests or personal relationships that could have appeared to influence the work reported in this paper.

Data availability

Data will be made available on request.

Acknowledgement

This work was developed within the scope of the projects HEALING - Healing of solid oxide fuel cell materials, POCI-01-0145-FEDER-032036 and project proMetheus – Research Unit on Materials, Energy and Environment for Sustainability, FCT - Ref. UID/05975/2020, financed by national funds through the FCT/MCTES.

References

[1] H. Su, Y.H. Hu, Progress in low-temperature solid oxide fuel cells with hydrocarbon fuels, Chem. Eng. J. 402 (2020) 126235, https://doi.org/10.1016/j.cej.2020.126235.
[2] T.S. Zhang, J. Ma, S.H. Chan, J.A. Kilner, Grain boundary conduction of Ce0.9Gd0.1O 2-δ ceramics derived from oxalate coprecipitation: effects of Fe loading and sintering temperature, Solid State Ionics 176 (2005) 377–384, https://doi.org/10.1016/j.ssi.2004.07.022.
[3] K.C. Anjaneya, G.P. Nayaka, J. Manjanna, G. Govindaraj, K.N. Ganesha, Preparation and characterization of Ce1-xSmxO 2-δ (x = 0.1-0.3) as electrolyte material for intermediate temperature SOFC, Solid State Sci. 26 (2013) 89–96, https://doi.org/10.1016/j.solidstatesciences.2013.09.015.
[4] S.A. Acharya, V.M. Gaikwad, S.W. D'Souza, S.R. Barman, Gd/Sm dopant-modified oxidation state and defect generation in nano-ceria, Solid State Ionics 260 (2014) 21–29, https://doi.org/10.1016/j.ssi.2014.03.008.
[5] T.S. Zhang, J. Ma, Y.J. Leng, Z.M., He, sintering, microstructure and grain growth of Fe-doped Ce 0.9Gd0.1O2-δ ceramics derived from oxalate coprecipitation, J. Cryst. Growth 274 (2005) 603–611, https://doi.org/10.1016/j.jcrysgro.2004.10.011.
[6] K. Sato, Grain-boundary structures associated with ionic transport in Gd-doped ceria nanostructured electrolyte, J. Phys. Chem. C 119 (2015) 5734–5738, https://doi.org/10.1021/acs.jpcc.5b00155.
[7] B. Steele, Appraisal of Ce1-ygdyO2-y/2 electrolyte for IT-SOFC operation at 500°C, Solid State Ionics 129 (2000) 95.
[8] T. Zhang, Z. Zeng, H. Huang, P. Hing, J. Kilner, Effect of alumina addition on the electrical and mechanical properties of Ce0.8Gd0.2O2-δ ceramics, Mater. Lett. 57 (2002) 124–129, https://doi.org/10.1016/S0167-577X(02)00717-6.
[9] D. Ivanova, V. Kharton, F. MarqueS, Silica-scavenging effects in ceria-based solid electrolytes, Bol. Soc. Esp. Ceram. 47 (2008) 201–206.
[10] N. Tian, J. Yu, Y. Deng, G. Li, X. Zhang, Electrical properties of Ce0.85Sm0.15O1.925-Fe2O3 electrolytes for IT-SOFCs, J. Alloys Compd. 655 (2016) 215–219, https://doi.org/10.1016/j.jallcom.2015.09.162.
[11] L. Ge, R. Li, S. He, H. Chen, L. Guo, Enhanced grain-boundary conduction in polycrystalline Ce 0.8Gd0.2O1.9 by zinc oxide doping: scavenging of resistive impurities, J. Power Sources 230 (2013) 161–168, https://doi.org/10.1016/j.jpowsour.2012.12.084.
[12] S. Xu, D. Li, K. Gao, Y. Yang, D. Xu, The effect of NiO addition on the grain boundary behavior and electrochemical performance of Gd-doped ceria solid electrolyte under different sintering conditions, J. Eur. Ceram. Soc. 37 (2017) 419–425.
[13] Y.H. Cho, P.S. Cho, G. Auchterlonie, D.K. Kim, J.H. Lee, D.Y. Kim, H.M. Park, J. Drennan, Enhancement of grain-boundary conduction in gadolinia-doped ceria by the scavenging of highly resistive siliceous phase, Acta Mater. 55 (2007) 4807–4815, https://doi.org/10.1016/j.actamat.2007.05.001.
[14] H. Bi, X. Liu, L. Zhu, J. Sun, S. Yu, H. Yu, L. Pei, Effect of MgO addition and grain size on the electrical properties of Ce0.9Gd0.1O1.95 electrolyte for IT-SOFCs, Int. J. Hydrog. Energy 42 (2017) 11735–11744, https://doi.org/10.1016/j.ijhydene.2017.02.110.
[15] Y. Zheng, S. He, L. Ge, M. Zhou, H. Chen, L. Guo, Effect of Sr on Sm-doped ceria electrolyte, Int. J. Hydrog. Energy 36 (2011) 5128–5135, https://doi.org/10.1016/j.ijhydene.2011.01.042.
[16] N. Jaiswal, D. Kumar, S. Upadhyay, O. Parkash, Effect of mg and Sr co-doping on the electrical properties of ceria-based electrolyte materials for intermediate temperature solid oxide fuel cells, J. Alloys Compd. 577 (2013) 456–462, https://doi.org/10.1016/j.jallcom.2013.06.094.
[17] D. Kashyap, P.K. Patro, R.K. Lenka, T. Mahata, P.K. Sinha, Effects of Gd and Sr co-doping in CeO2 for electrolyte application in solid oxide fuel cell (SOFC), Ceram. Int. 40 (2014) 11869–11875, https://doi.org/10.1016/j.ceramint.2014.04.021.
[18] Z. Gao, X. Liu, B. Bergman, Z. Zhao, Enhanced ionic conductivity of Ce 0.8Sm 0.2O 2-δ by Sr addition, J. Power Sources 208 (2012) 225–231, https://doi.org/10.1016/j.jpowsour.2012.01.001.
[19] P.S. Cho, S.B. Lee, D.S. Kim, J.H. Lee, D.Y. Kim, H.M. Park, Improvement of grain-boundary conduction in gadolinia-doped ceria by the addition of CaO, Electrochem. Solid-State Lett. 9 (2006), https://doi.org/10.1149/1.2214235.
[20] S. Preethi, K.S. Babu, Divalent cations modified grain boundary scavenging in samarium doped ceria electrolyte for solid oxide fuel cells, J. Alloys Compd. 792 (2019) 1068–1078, https://doi.org/10.1016/j.jallcom.2019.04.062.
[21] S.-Y. Park, P.-S. Cho, S.B. Lee, H.-M. Park, J.-H. Lee, Improvement of grain-boundary conduction in SiO2-doped GDC by BaO addition, J. Electrochem. Soc. 156 (2009) B891, https://doi.org/10.1149/1.3139074.
[22] X. Sun, T. Wang, D. Yan, G. Zhang, D. Wang, C. Wang, R. Liu, Insight into impurity scavenging effect of gadolinium-doped ceria electrolytes, Ceram. Int. 46 (2020) 7218–7222, https://doi.org/10.1016/j.ceramint.2019.11.216.
[23] L. Ge, Q. Ni, G. Cai, T. Sang, L. Guo, Improving SiO2 impurity tolerance of Ce0.8Sm0.2O1.9: synergy of CaO and ZnO in scavenging grain-boundary resistive phases, J. Power Sources 324 (2016) 582–588, https://doi.org/10.1016/j.jpowsour.2016.05.135.
[24] X. Song, D. Liao, Z. Lian, Feng Chen, K. Peng, Effects of monovalent alkali metals on grain boundary conductivity and electrochemical properties of gadolinia-doped ceria electrolyte, Ceram. Int. 47 (2021) 18773–18782, https://doi.org/10.1016/j.ceramint.2021.03.212.
[25] D.P. Fagg, J.C.C. Abrantes, D. Pérez-Coll, P. Núñez, V.V. Kharton, J.R. Frade, The effect of cobalt oxide sintering aid on electronic transport in Ce0.80Gd0.20O2-δ electrolyte, Electrochim. Acta 48 (2003) 1023–1029, https://doi.org/10.1016/S0013-4686(02)00816-2.
[26] Y. Lykhach, T. Staudt, R. Streber, M.P.A. Lorenz, A. Bayer, H.P. Steinrück, J. Libuda, CO 2 activation on single crystal based ceria and magnesia/ceria model catalysts, Eur. Phys. J. B. 75 (2010) 89–100, https://doi.org/10.1140/epjb/e2010-00110-x.
[27] J. and L.D. Kim, The effect of multiple doping on electrical conductivity of GDC electrolyte, Korean J. Chem. Eng. 19 (2002) 421–424.
[28] R.D. Shannon, Revised effective ionic radii and systematic studies of interatomic distances in halides and chalcogenides, Acta Crystallogr. Sect. A. 32 (1976) 751–767, https://doi.org/10.1107/S0567739476001551.
[29] M. Schaube, R. Merkle, J. Maier, Interdependence of point defects and reaction kinetics: CO and CH4 oxidation on ceria and zirconia, J. Phys. Chem. C 124 (2020) 18544–18556, https://doi.org/10.1021/acs.jpcc.0c03256.
[30] J.C.C. Abrantes, J.R. Frade, ISA-Impedance Spectroscopy Analyser, Software Package, 2001.
[31] D. Pérez-Coll, P. Núñez, J.R. Frade, J.C.C. Abrantes, Conductivity of CGO and CSO ceramics obtained from freeze-dried precursors, Electrochim. Acta 48 (2003) 1551–1557, https://doi.org/10.1016/S0013-4686(03)00027-6.
[32] G.M. Christie, F.P.F. Van Berkel, Microstructure - ionic conductivity relationships in ceria-gadolinia electrolytes, Solid State Ionics 83 (1996) 17–27, https://doi.org/10.1016/0167-2738(95)00155-7.
[33] H.J. Avila-Paredes, K. Choi, C.T. Chen, S. Kim, Dopant-concentration dependence of grain-boundary conductivity in ceria: a space-charge analysis, J. Mater. Chem. 19 (2009) 4837–4842, https://doi.org/10.1039/b904583j.
[34] C. Korte, A. Peters, J. Janek, D. Hesse, N. Zakharov, Ionic conductivity and activation energy for oxygen ion transport in superlattices-the semicoherent multilayer system YSZ (ZrO2 + 9.5 Mol% Y2O3)/Y2O3, Phys. Chem. Chem. Phys. 10 (2008) 4623–4635, https://doi.org/10.1039/b801675e.
[35] M. Nakayama, M and Martin, first-principles study on defect chemistry and migration of oxide ions in ceria doped with rare-earth cations, Phys. Chem. Chem. Phys. 11 (2009) 3241–3249, https://doi.org/10.1039/b900162.
[36] S.W. Kim, Y. Lee, G.M. Choi, Electrical conductivity of Gd-doped ceria film at low temperatures (300-500 °c), Solid State Ionics 262 (2014) 411–415, https://doi.org/10.1016/j.ssi.2014.01.014.
[37] P. Sudarsan, S.B. Krishna Moorthy, Synergistic effect of lithium and calcium for low temperature densification and grain boundary scavenging in samarium doped ceria electrolyte, Mater. Chem. Phys. 238 (2019) 121900, https://doi.org/10.1016/j.matchemphys.2019.121900.
[38] X. Guo, R. Waser, Electrical properties of the grain boundaries of oxygen ion conductors: acceptor-doped zirconia and ceria, Prog. Mater. Sci. 51 (2006) 151–210, https://doi.org/10.1016/j.pmatsci.2005.07.001.
[39] D. Yan, X. Liu, X. Bai, L. Pei, M. Zheng, C. Zhu, D. Wang, W. Su, Electrical properties of grain boundaries and size effects in samarium-doped ceria, J. Power Sources 195 (2010) 6486–6490, https://doi.org/10.1016/j.jpowsour.2010.04.034.